

CASE REPORT

Favorable response to immunotherapy in a pancreatic neuroendocrine tumor with temozolomide-induced high tumor mutational burden

Yanshuo Cao¹  | Yutong Ma²  | Jiangyuan Yu³ | Yu Sun⁴ | Tingting Sun⁵ | Yang Shao^{5,6} | Jie Li¹ | Lin Shen^{1,7} | Ming Lu¹

¹ Department of Gastrointestinal Oncology, Key Laboratory of Carcinogenesis and Translational Research (Ministry of Education/Beijing), Peking University Cancer Hospital & Institute, Beijing 100142, P. R. China

² Translational Medicine Research Institute, Geneseeq Technology Inc., Toronto M5T1K5, Canada

³ Department of Nuclear Medicine, Peking University Cancer Hospital & Institute, Key Laboratory of Carcinogenesis and Translational Research (Ministry of Education/Beijing), Beijing 100142, P. R. China

⁴ Department of Pathology, Key Laboratory of Carcinogenesis and Translational Research (Ministry of Education/Beijing), Peking University Cancer Hospital & Institute, Beijing 100142, P. R. China

⁵ Nanjing Geneseeq Technology Inc., Nanjing, Jiangsu 210032, P. R. China

⁶ School of Public Health, Nanjing Medical University, Nanjing, Jiangsu 210029, P. R. China

⁷ Department of Early Drug Development Center, Peking University Cancer Hospital & Institute, Key Laboratory of Carcinogenesis and Translational Research (Ministry of Education/Beijing), Beijing 100142, P. R. China

Correspondence

Ming Lu, MD, Department of Gastrointestinal Oncology, Peking University Cancer Hospital & Institute; Key Laboratory of Carcinogenesis and Translational Research (Ministry of Education/Beijing), Beijing 100142, P. R. China.
Email: qiminglu_mail@126.com

Funding information

National Key Research and Development Program of China, Grant/Award Number: 2017YFC0908404

Abstract

Neuroendocrine neoplasm of the pancreas is a rare tumor with limited treatment options. Among such tumors, treatment for pancreatic neuroendocrine tumor (PanNET) G3 is the most difficult. Temozolomide (TMZ) is commonly used to treat PanNET. However, TMZ may cause tumor gene alkylation, which induces drug resistance and rapid disease progression. Herein, we present a case of a female who was diagnosed with PanNET G3 and achieved a partial response to toripalimab, an anti-programmed cell death-ligand 1 (anti-PD-L1) monoclonal antibody, after multiple cycles of TMZ treatment. Genomic profiling revealed that compared with the patient's samples collected at baseline, the post-TMZ-treatment samples had markedly higher levels of tumor mutational burden (TMB) associated with characteristic alkylating mutational signature representing a positive correlation with favorable response to anti-PD-1 treatment. In

Abbreviations: AF, allele frequency; ATRX, ATRX chromatin remodeler; CAPTEM, capecitabine/temozolomide; ctDNA, circulating tumor DNA; FACETS, fraction and allele-specific copy number estimates from tumor sequencing; ICIs, immune checkpoint inhibitors; IHC, immunohistochemical; LOH, loss of heterozygosity; NGS, next-generation sequencing; PanNECs, pancreatic neuroendocrine carcinomas; PanNENs, pancreatic neuroendocrine neoplasms; PanNETs, pancreatic neuroendocrine tumors; PD, progressive disease; PD-1, programmed death receptor-1; PET/CT, positron emission tomography/computed tomography; PR, partial response; RBI, RB transcriptional corepressor 1; SSA, somatostatin analogs; SSTR, somatostatin receptor; TAE, tumor arterial embolization; TMB, tumor mutational burden; BMI, body mass index

This is an open access article under the terms of the [Creative Commons Attribution-NonCommercial-NoDerivs](https://creativecommons.org/licenses/by-nc-nd/4.0/) License, which permits use and distribution in any medium, provided the original work is properly cited, the use is non-commercial and no modifications or adaptations are made.

© 2020 The Authors. *Cancer Communications* published by John Wiley & Sons Australia, Ltd. on behalf of Sun Yat-sen University Cancer Center

addition, we observed a germline truncating mutation of *MUTYH* (W156*) that was considered to be pathogenic and potentially conferred to genomic instability. This case suggests that anti-PD-1 therapy could be a treatment option for PanNET patients with increased TMB after TMZ-based treatment.

KEYWORDS

gene expression profiling, mutational signature, neuroendocrine tumors, programmed cell death 1 receptor, temozolomide, tumor mutational burden

1 | INTRODUCTION

Pancreatic neuroendocrine neoplasms (PanNENs) are morphologically grouped into well-differentiated neuroendocrine tumors (PanNETs) and poorly-differentiated neuroendocrine carcinomas (PanNECs) [1]. NETs are graded as G1, G2, or G3 based on their proliferative activity [1]. Besides immunohistochemistry (IHC) tests, genetic tests also play important roles in PanNENs diagnosis [2].

Treatments for unresectable or metastatic PanNENs depend on the tumor pathology [3], while the treatment for well-differentiated PanNET G3 follows that of PanNET G2, i.e. use of the capecitabine/temozolomide (CAPTEM) regimen [4], and second-line treatments including everolimus [5] and sunitinib [6]. For poorly-differentiated PanNET G3, platinum-based chemotherapy is often preferred [7]. Currently, immunotherapy is not yet approved for PanNETs as clinical trial data have suggested an unpromising response [8], but recently a 75% objective response rate was reported in NET with high tumor mutational burden (TMB) (≥ 9.9 mutations/Mb) [9].

Here, we present the case of a patient diagnosed with metastatic PanNET G3 who had characteristic gene mutations along multiple lines of treatments.

2 | CASE REPORT

A 49-year-old female (Figure 1A) (BMI, body mass index; 16.82) presenting epigastric pain underwent magnetic resonance imaging, which showed a tumor at the pancreatic tail, with enlarged regional lymph nodes, and tumor thrombosis within the portal and splenic vein (Figure 1B). An ultrasound-guided biopsy of the pancreatic tumor revealed a well-differentiated NET (Figure 2A) with high proliferation (Ki-67 index: 35%+; Supplementary Table S1). ^{68}Ga -DOTATATE-PET/CT showed a high expression of the somatostatin receptor (SSTR) in all lesions. After a multi-disciplinary team discussion, the patient was diagnosed with PanNET G3 on January 22, 2018. Comorbidity included hyperlipidemia and was treated with atorvastatin.

First-line treatment with six cycles of CAPTEM plus somatostatin analogs (SSA) (capecitabine 1 g Qd 1.5 g Qn, d1-14; TMZ 0.26 g Qd d10-14; SSA 30 mg d1 Q28d) led to a partial response (PR) and relief of symptoms. Adverse events included grade 2 leukopenia and thrombocytopenia. Following that, 8 cycles of capecitabine plus SSA were administered as maintenance therapy and follow-up CT scans revealed stable disease (Figure 1C). However, after the tenth cycle of maintenance treatment, multiple new liver lesions were discovered ranging from 5 mm to 28 mm (Figure 1D). Given the favorable response of the first-line treatment, two cycles of CAPTEM plus SSA were re-challenged, but both ^{68}Ga -DOTATATE and ^{18}F FDG-PET/CT showed progressive disease (PD) (Figure 1E). An ultrasound-guided biopsy of the liver lesions was performed and showed higher proliferation (Ki-67 index: 80%+; Supplementary Table S1) compared to the primary PanNET (Figure 2B). Since the pancreatic lesion remained stable, re-biopsy was avoided to reduce unnecessary injuries.

Tissue samples of the primary PanNET, liver metastasis and plasma samples collected at baseline and after PD (Figure 1A) were subjected to targeted next-generation sequencing (NGS; Nanjing Geneseeq Technology Inc., Nanjing, Jiangsu, China) for 425 cancer-relevant genes, as described previously [10]. Circulating tumor DNA (ctDNA) mutation positivity increased upon PD (Figure 3A), and the TMB in PD plasma and liver metastasis samples increased dramatically (Figure 1A), and was found to be associated with the alkylation-induced mutational signature, Signature 11 (Figure 3B), similar to a previous report [11]. However, the mutation signature could not be identified in baseline samples due to the low mutation number (< 5 mutations). Moreover, a germline heterozygous nonsense mutation of *MUTYH* (p.W156*) was identified by NGS in all plasma collected samples (Supplementary Table S2). Fraction and allele-specific copy number estimates from tumor sequencing [12] analysis showed that loss of heterozygosity (LOH) was common in the primary PanNET, including chromosome 1p, where the *MUTYH* gene is located (Figure 3C). However, due to

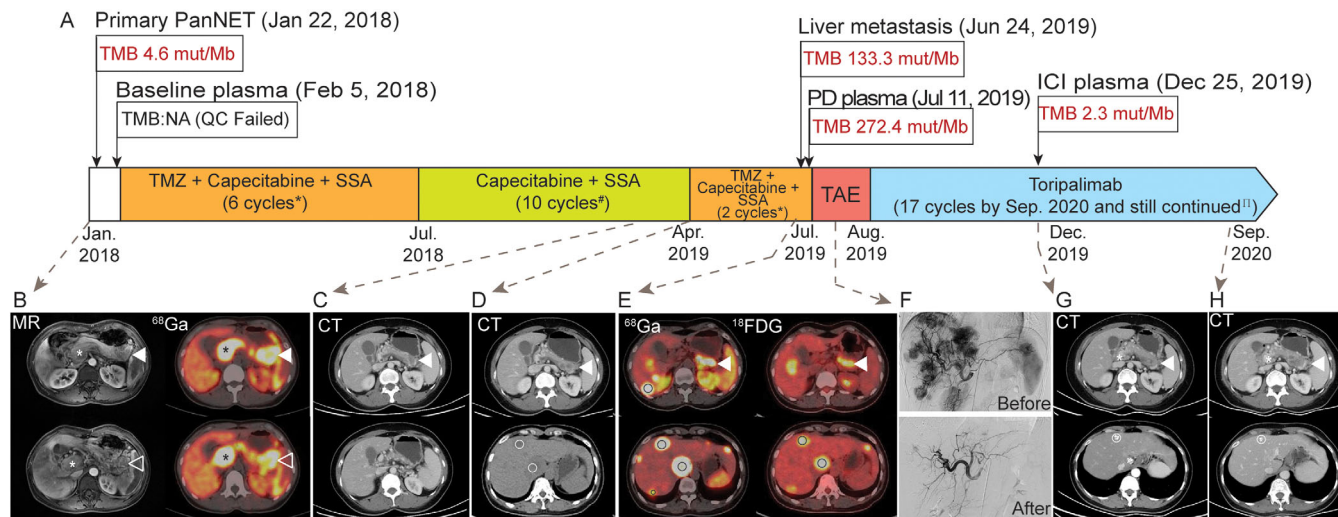


FIGURE 1 Chronological presentation of the patient's clinical history and medical treatment. (A) Medical history of the patient. (B) MR: fullness of the pancreatic body and tail, with a mass of long T2 signal and uneven enhancement, 25 mm × 23 mm in size (solid arrowhead: primary pancreatic tumor), without a clear demarcation line between the tumor, the spleen, and the wall of the gastric body. The hollow arrowheads indicate multiple enlarged adenopathies adjacent to the pancreatic mass. The asterisk points to the tumor thrombosis characterized by the dilation of the portal vein and splenic vein, with massive long T1 and uneven long T2 signal inside (maximum diameter of 33 mm). ⁶⁸Ga: A mass at the pancreatic body and tail, with multiple adenopathies; tumor thrombosis within the portal vein and splenic vein. All lesions showed a high expression of SSTR (SUVmax, 37.6). (C) CT: A locally invasive tumor mass at the level of the pancreatic body and tail (solid arrowhead: primary pancreatic tumor), 23 mm × 20 mm in size. (D) CT: A locally invasive tumor mass at the level of the pancreatic body and tail (solid arrowhead: pancreatic primary), 24 mm × 20 mm in size. Multiple intrahepatic foci of varying sizes and low density (hollow circles: liver metastases), with the largest one 28 mm × 24 mm in size, and the smallest one being 5 mm in size. (E) ⁶⁸Ga and ¹⁸FDG: A mass at the level of the pancreatic body and tail, with multiple intrahepatic foci of varying sizes. All lesions show a high expression of SSTR (SUVmax 33.1) and moderate ¹⁸FDG uptake (SUVmax 7.2). (F) Hepatic arteriograms before and after transarterial embolization show that the feeding artery of the tumor was completely blocked. (G) CT: A locally invasive tumor mass at the level of the pancreatic body and tail (solid arrowhead: primary pancreatic tumor), 33 mm × 17 mm in size. Filling defect at the level of the main portal vein and splenic vein (asterisk: tumor thrombosis). Multiple liver nodules show iodine deposition which was caused by TAE (hollow circle: liver metastasis), the largest one 12 mm × 10mm in size. (H) CT: A locally invasive tumor mass at the level of the pancreatic body and tail (solid arrowhead: primary pancreatic tumor), 33 mm × 17 mm in size. Filling defect at the level of the main portal vein and splenic vein (asterisk: tumor thrombosis). Multiple liver nodules show iodine deposition (hollow circle: liver metastasis), the largest of which was 10 mm × 9 mm in size. Detailed dosages of medications: *Capecitabine 1 g/m² (1 g Qd 1.5 g Qn), d1-14; TMZ 0.26 g Qd d10-14; SSA 30 mg im d1 Q28d; # Capecitabine 1 g/m² (1 g Qd 1.5 g Qn), d1-14; SSA 30 mg im d1 Q28d; ^{II} Toripalimab 240 mg iv d1 Q21d. Accumulated TMZ dose 7.54 g/m². Abbreviations: PanNET: pancreatic neuroendocrine tumor; TMB: tumor mutational burden; NA: not applicable; QC: quality control; TMZ: temozolomide; SSA: somatostatin analogs; PD: progressive disease; ICI: immune checkpoint inhibitor; MR: magnetic resonance; ⁶⁸Ga: Ga-68 DOTATATE positron emission tomography/computed tomography; SSTR: somatostatin receptor; CT: computed tomography; ¹⁸FDG: F-18 fluorodeoxyglucose positron emission tomography/computed tomography; TAE: tumor arterial embolization

the low amount of ctDNA in the baseline plasma sample, we could not detect any mutations above the 0.5% cut-off adopted for the analysis, which was determined by the applied targeted NGS.

As liver metastasis was the major tumor burden, tumor arterial embolization (TAE) was applied to the liver lesions (Figure 1F). The patient then received toripalimab (Shanghai Junshi Bioscience Co., Ltd in China), a programmed death receptor-1 (PD-1) monoclonal antibody, 240 mg every 3 weeks, and achieved a PR (Figure 1G) by the follow-up visit in December 2019. The TMB (Figure 1A) and mutational allele frequency (AF; Figure 3A) were dramatically reduced after immunotherapy (median AF of PD plasma

vs ICI plasma: 5.49% vs 0.35%). The anti-PD-1 treatment is still ongoing and has been administrated for 17 cycles. As of the last follow-up on September 3, 2020 (BMI 17.58), no significant adverse effects were observed and CT scans revealed stable diseases at the primary PanNET and liver metastases (Figure 1H).

3 | DISCUSSION

Pathological diagnosis of the primary PanNET in this case report was challenging as it contained features of both NETs and NECs. The evidence of PanNET includes

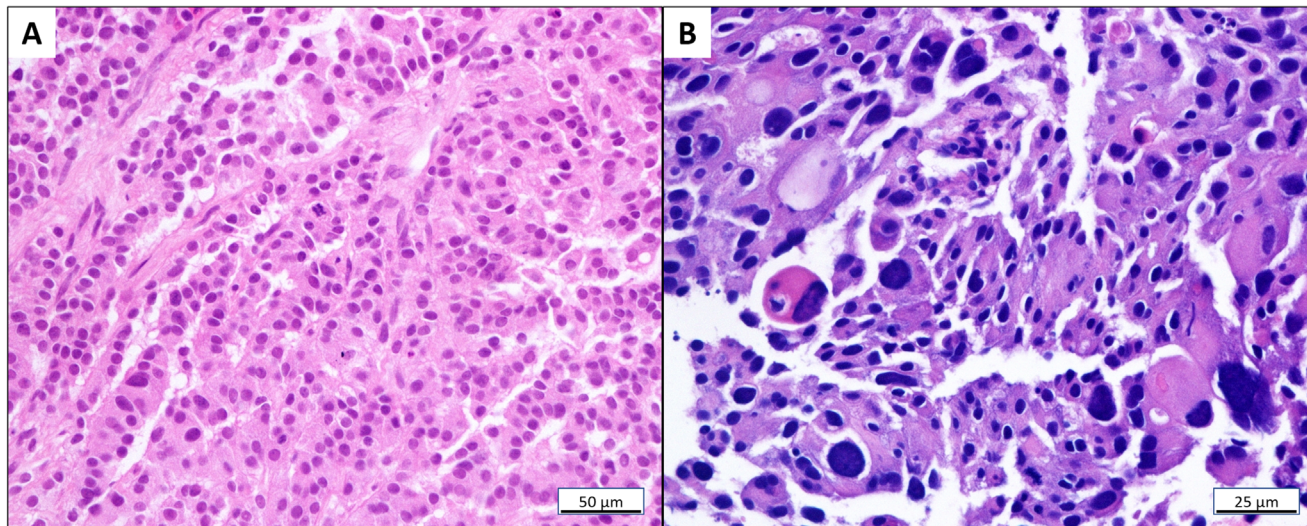


FIGURE 2 The hematoxylin and eosin stain of (A) PanNET primary and (B) liver metastasis. (A) PanNET primary tumor at baseline (magnification: $\times 200$) exhibits an organoid and trabecular architecture, a regular intratumoral vascular pattern, abundant granular cytoplasm, and stippled nuclei with inconspicuous nucleoli; (B) liver metastasis (magnification: $\times 400$) exhibits a composition of large nests of cells with prominent atypia. Abbreviations: PanNET: pancreatic neuroendocrine tumor

pathological morphology, Ki-67 index, SSTR2 expression, and the presence of *ATRX* mutation. However, the IHC and NGS results revealed the loss of *RB1* in the primary pancreatic tumor and liver metastasis, which is a feature of PanNETs [2]. To our knowledge, this is the first case reporting the co-existence of mutations in the *ATRX* and *RB1* genes, which are routinely used to distinguish PanNETs and PanNETCs. However, the liver lesion was poorly differentiated with a high Ki-67 index that resembled NECs, suggesting a possible but rare transformation from NET G3 to NEC [1].

NGS analysis contributed to the pathogenic diagnosis of this case, as we identified an inactivating germline mutation in the base-excision-repair gene *MUTYH* which was reported as a novel pathogenesis in PanNETs [14]. However, whether this monoallelic germline *MUTYH* mutation is the trigger for the genome-wide LOH remains to be determined. To illustrate the biological mechanisms causing high TMB in PD samples, we performed mutational signature analysis based on the combinations of characteristic mutation types. Signature 11, which is associated with alkylation due to TMZ treatment, may have contributed the most to the elevated TMB in this case [15]. However, the high TMB might also be attributable to other unknown mechanisms as we only performed mutational signature analysis for the samples with TMB > 10 mutations/Mb to ensure reliability. Due to different DNA extraction techniques and insufficient ctDNA release, the discordance between tissue TMB and blood TMB was reported [13] and could explain the inconsistent TMB values detected in the liver tissue and PD plasma.

In conclusion, we described a PanNET G3 case, with increasing TMB induced by TMZ-related alkylation, which presented a favorable clinical response to anti-PD-1 treatment. Based on the described observations, we suggest that the use of ICIs should be further explored as a treatment option for PanNET patients with increased TMB following TMZ treatment.

DECLARATIONS

ETHICS APPROVAL AND CONSENT TO PARTICIPATE

The study was approved by the ethics committee of Peking University Cancer Hospital & Institute. Written consent was obtained from the patient.

CONSENT FOR PUBLICATION

Not Applicable

AVAILABILITY OF DATA AND MATERIALS

Additional data and materials related to the genetic tests, pathologic reports, treatment information, and images are available for review upon reasonable request.

COMPETING INTERESTS

Yutong Ma is an employee of Geneseeq Technology Inc., Canada. Tingting Sun and Yang W. Shao are employees of Nanjing Geneseeq Technology Inc., P. R. China. The remaining authors have no competing interests to declare.

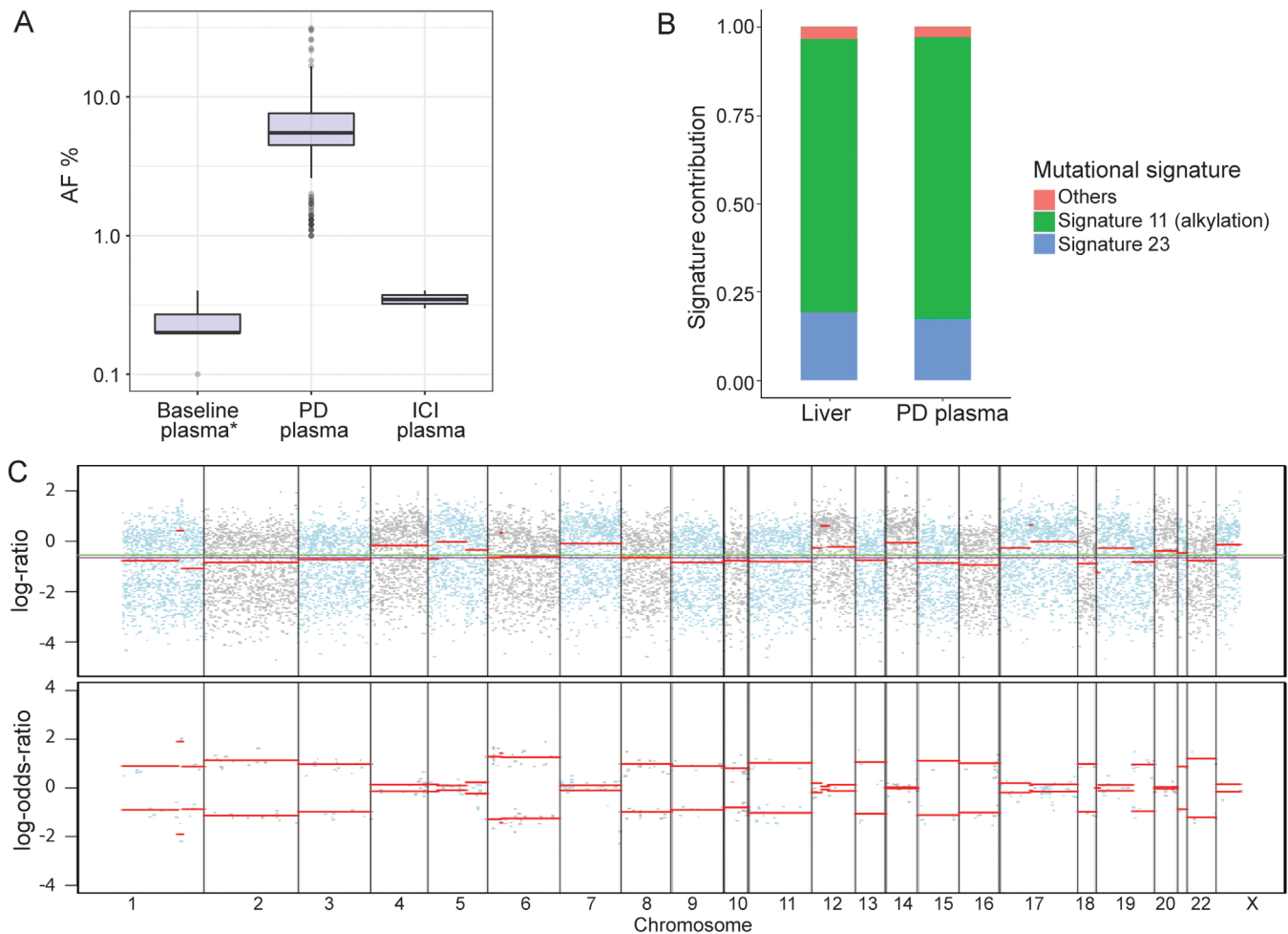


FIGURE 3 Disease surveillance and monitoring with NGS. (A) Mutational AF of ctDNA in plasma samples collected before TMZ treatment (baseline), after PD, and after ICI. The extracted amount of cell-free DNA from each plasma sample was 16.2 ng/mL at baseline, 13.5 ng/mL after PD, and 13.7 ng/mL after ICI. The AF in the baseline plasma was below the 0.5% cut-off for quality control which was determined as the limit of detection of plasma from healthy controls. (B) Mutational signature analysis of NGS data from liver metastasis and plasma samples after the failure of first-line TMZ treatment. Signature 11, an alkylation-induced signature, was the most dominant, followed by Signature 23 whose etiology remains unknown. (C) Integrated visualization of FACETS analysis of NGS data from the primary PanNET sample indicates genome instability with the losses of multiple chromosomes. The top panel displays the total copy number log-ratio which is computed from the total read count in the tumor versus normal tissues at all panel-covered genomic regions. The bottom panel displays the allele-specific log-odds-ratio of the variant allele read counts in the tumor versus normal samples. The blue and gray dots are the observed values, and the red bars are estimates. The chromosomes are separated by lines and alternated by blue and gray dots. Abbreviations: NGS: next-generation sequencing; AF: allele frequency; ctDNA, circulating tumor DNA; TMZ: temozolomide; PD: progressive disease; ICI: immune checkpoint inhibitor; FACETS: fraction and allele-specific copy number estimates from tumor sequencing; PanNET, pancreatic neuroendocrine tumor

AUTHORS' CONTRIBUTIONS

ML, JL, and LS contributed to the conception of the work.

YSC contributed to the acquisition and interpretation of data, drafting, and revising the manuscript.

YTM contributed to the analysis of the genetic test results and revision of the manuscript.

JYY contributed to the interpretation of the nuclear medicine results and images.

YS contributed to the interpretation of the pathology results and images.

TTS and YS contributed to the collection of the genetic test results.

ACKNOWLEDGMENTS

We sincerely thank the patient for supporting our work. We thank Drs. Yong Cui, Xiaolei Gu, and Peng Liu for helping to prepare and interpreting the radiology results and images. We also thank Drs. Qiuxiang Ou and Hua Bao for help interpreting the genetic test results.

ORCID

Yanshuo Cao  <https://orcid.org/0000-0003-4030-8600>Yutong Ma  <https://orcid.org/0000-0002-0622-2793>

REFERENCES

- Rindi G, Klimstra DS, Abedi-Ardekani B et al. A common classification framework for neuroendocrine neoplasms: an International Agency for Research on Cancer (IARC) and World Health Organization (WHO) expert consensus proposal. *Mod Pathol*. 2018;31:1770-1786.
- Tang LH, Basturk O, Sue JJ, Klimstra DS. A Practical Approach to the Classification of WHO Grade 3 (G3) Well-differentiated Neuroendocrine Tumor (WD-NET) and Poorly Differentiated Neuroendocrine Carcinoma (PD-NEC) of the Pancreas. *Am J Surg Pathol*. 2016;40:1192-1202.
- Rinke A, Muller HH, Schade-Brittinger C et al. Placebo-controlled, double-blind, prospective, randomized study on the effect of octreotide LAR in the control of tumor growth in patients with metastatic neuroendocrine midgut tumors: a report from the PROMID Study Group. *J Clin Oncol*. 2009;27:4656-4663.
- Fine RL, Gulati AP, Krantz BA et al. Capecitabine and temozolomide (CAPTEM) for metastatic, well-differentiated neuroendocrine cancers: The Pancreas Center at Columbia University experience. *Cancer Chemother Pharmacol*. 2013;71:663-670.
- Yao JC, Shah MH, Ito T et al. Everolimus for advanced pancreatic neuroendocrine tumors. *N Engl J Med*. 2011;364:514-523.
- Faivre S, Niccoli P, Castellano D et al. Sunitinib in pancreatic neuroendocrine tumors: updated progression-free survival and final overall survival from a phase III randomized study. *Ann Oncol*. 2017;28:339-343.
- Yamaguchi T, Machida N, Morizane C et al. Multicenter retrospective analysis of systemic chemotherapy for advanced neuroendocrine carcinoma of the digestive system. *Cancer Sci*. 2014;105:1176-1181.
- Yao J, Strosberg J, Fazio N et al. 1308O Activity & safety of spartalizumab (PDR001) in patients (pts) with advanced neuroendocrine tumors (NET) of pancreatic (Pan), gastrointestinal (GI), or thoracic (T) origin, & gastroenteropancreatic neuroendocrine carcinoma (GEP NEC) who have progressed on prior treatment (Tx). *Annals of Oncology*. 2018;29.
- Lu M, Zhang P, Zhang Y et al. Efficacy, Safety, and Biomarkers of Toripalimab in Patients with Recurrent or Metastatic Neuroendocrine Neoplasms: A Multiple-Center Phase Ib Trial. *Clin Cancer Res*. 2020;26:2337-2345.
- Shu Y, Wu X, Tong X et al. Circulating Tumor DNA Mutation Profiling by Targeted Next Generation Sequencing Provides Guidance for Personalized Treatments in Multiple Cancer Types. *Scientific Reports*. 2017;7:583.
- Kucab JE, Zou X, Morganello S et al. A Compendium of Mutational Signatures of Environmental Agents. *Cell*. 2019;177:821-836 e816.
- Shen R, Seshan VE. FACETS: allele-specific copy number and clonal heterogeneity analysis tool for high-throughput DNA sequencing. *Nucleic Acids Res*. 2016;44:e131.
- Fang W, Ma Y, Yin JC et al. Combinatorial assessment of ctDNA release and mutational burden predicts anti-PD(L)1 therapy outcome in nonsmall-cell lung cancer. *Clin Transl Med*. 2020;10:331-336.
- Scarpa A, Chang DK, Nones K et al. Whole-genome landscape of pancreatic neuroendocrine tumours. *Nature*. 2017;543:65-71.
- Saini N, Sterling JF, Sakofsky CJ et al. Mutation signatures specific to DNA alkylating agents in yeast and cancers. *Nucleic Acids Res*. 2020;48:3692-3707.

SUPPORTING INFORMATION

Additional supporting information may be found online in the Supporting Information section at the end of the article.

How to cite this article: Cao Y, Ma Y, Yu J, et al. Favorable response to immunotherapy in a pancreatic neuroendocrine tumor with temozolomide-induced high tumor mutational burden. *Cancer Commun*. 2020;1-6. <https://doi.org/10.1002/cac2.12114>